*Short Communication*

# Investigation of Pt/SnO₂/C Catalyst for Dimethyl Ether Oxidation in DDFC

*Lehong Xing[1,2,*], Yixin Wang[1], Chao Sui[1], Na Zhang[2]*

[1] College of Chemistry and Chemical Engineering, Mu Danjiang Normal University, Mu Danjiang 157012 ,China
[2] School of Chemical Engineering and Technology, Harbin Institute of Technology, No. 92, West Da-Zhi Street, Harbin 150001 China
[*]E-mail: xinglehonghit@126.com

The performance of Pt loading on $SnO_2$/C support catalyst has been investigated for dimethyl ether (DME) oxidation in direct dimethyl ether fuel cells (DDFCs). The transmission electron micrograph (TEM) tests show that the sizes of Pt particles loading on different supports ($SnO_2$/C and XC-72 carbon black) are nearly the same (3.2 nm). The cyclic voltammograms results reveal that Pt/$SnO_2$/C shows higher activity towards DME oxidation. DME prefers to be adsorbed on Pt/$SnO_2$/C surface. $SnO_2$ can adsorb $OH_{ads}$ species which benefit to reduce the Pt poisoning effect. The maximum power density of DDFC has been enhanced by using Pt/$SnO_2$/C as the anodic catalyst. The electrochemical active surfaces (*EAS*) of different anodes are nearly the same. That is, the improvement of DDFC performance can be attributed to the enhanced activity of anode catalyst.

**Keywords:** Direct dimethyl ether fuel cell; Dimethyl ether; Anode catalyst; Supports; Pt/$SnO_2$/C

## 1. INTRODUCTION

At present, traditional energy resources such as coal, natural gas and oil are nearly exhausted. Fuel cells such as proton exchange membrane fuel cells (PEMFCs) and direct methanol fuel cells (DMFCs) have been widely studied to solve the potential energy crisis problems [1-3]. However, PEMFCs and DMFCs still have some obstacles which hinder their broad applications [4,5]. Dimethyl ether (DME) is a new attractive fuel for PEMFCs which has many advantages. The energy density of DME is high and its toxicity is low. DME has low fuel crossover effect [6]. The transportation of DME is convenient because it can be liquefied easily [7]. However, the major obstacle limits the performance of direct dimethyl ether fuel cell (DDFC) is the relatively slow kinetics of anodic DME oxidation. The improvement of catalyst activity towards DME oxidation is very important for DDFC [8]. Pt and Pt-M

alloys are prominent catalysts for DDFCs [9]. Recently, metallic oxides have attracted increasing attention for catalytic researchers for their excellent co-catalyst effect [10]. In particular, tin dioxide ($SnO_2$) exhibits many advantages. $SnO_2$ shows high stability at anode. $SnO_2$ can adsorb sufficient $OH_{ads}$ species. These $OH_{ads}$ benefit to oxidize the poisoning intermediates generated during DME anodic oxidation reaction and release Pt active sites [11]. In addition, $SnO_2$ and $SnO_2$ based nanomaterials have been used as catalyst supports. The catalytic activity has been enhanced because of the strong metal-support interaction [12-14].

In this study, the aim of work is to utilize $SnO_2$ loaded on XC-72 carbon black as the catalyst support to enhance the DME oxidation activity. Firstly, homemade nano $SnO_2/C$ composites are synthesized by hydrolysis method. Then, nano Pt particles are deposited on the $SnO_2/C$ composites. The effects of catalyst supports on DME oxidation and the performance of DDFC have been discussed based on physical characterizations and electrochemical tests results.

## 2. EXPERIMENTAL

### 2.1. Preparation of catalyst

Preparation of nano $SnO_2/C$ [15]: 64 mg of Dihydrate tin (II) halide were dissolved in the solution which was composed of 25 ml ethylene glycol (EG) and 1 ml water. 200 mg of carbon black (Vulcan, XC-72) was dispersed in another 25 ml EG. The two obtained solutions were mixed in a three-neckround-bottom flask. The mixture was kept at 190 °C for 3 h under stirring. Then, the mixture was cooled down to about 25 °C. The products were filtered and washed 3 times. At last, the resulting powders were dried under vacuum condition. The theoretical content of $SnO_2$ in prepared supports was 20 wt. %.

Preparation of nano Pt based catalyst [15]: A 2.65 mL of $H_2PtCl_6$ - EG solution was diluted by 200 mL EG. The solution was adjusted to pH≈12 using NaOH-EG solution. An 80 mg of supports were dispersed into the solution under ultrasonic treatment for 0.5 h. Then the solution was refluxed for 4 h at 140 °C. The solution was cooled down to about 25 °C under stirring. Then the solution was adjusted to pH≈3 using 0.1 M $HNO_3$ solution. The homemade catalyst was washed 3 times, and then dried for 4 h at 80 °C under vacuum condition. As comparison, the 20 mass % Pt/C was prepared as reference catalyst.

### 2.2. MEA fabrication

The MEAs (5 $cm^2$) were prepared by the traditional methods which have been reported previously [16]. The wet-proofed Toray carbon papers were used as anode diffusion layers. The PTFE content of anode diffusion layers was 18 wt.%. The wet-proofed carbon papers coated with 1 mg $cm^{-2}$ of carbon black and PTFE were used as the cathode diffusion layers. The PTFE content of cathode diffusion layers was 30 wt.%. The anodic catalysts of different MEAs were $Pt/SnO_2/C$ and Pt/C, respectively. The cathodic catalysts of different MEAs were both Pt/C. In catalyst layer, the Pt loading was 2 mg $cm^{-2}$, and Nafion content was 20 wt.%.

## 2.3. Physical characterization

The morphology of catalyst was characterized by TEM (Hitachi H-7650). To examine and measure the content of $SnO_2$ in $Pt/SnO_2/C$, the chemical composition of the $Pt/SnO_2/C$ was analyzed by EDAX techniques (HITACHIS-4700). The IR spectra (ThermoFisher- is10) were used to examine the $OH_{ads}$ species on $SnO_2$ surface.

## 2.4. Electrochemical measurements

### 2.4.1 Cyclic voltammetry

Cyclic voltammetry (CV) measurements were conducted to evaluate anodic *EAS* [17]. During the test, humidified $N_2$ was pumped to the anode and humidified $H_2$ was pumped to the cathode. The cathode was used as a dynamic hydrogen electrode (DHE). The flow rate of $N_2$ and $H_2$ were both 200 mL min$^{-1}$. The CV measurements were performed from 0.05 V to 1.2 V (VS DHE). The scan rate was 0.01 V s$^{-1}$. The *EAS* of anodic catalyst could be calculated through Eq.(1):

$$EAS_H = \frac{Q_H}{[Pt] \times 0.21} \tag{1}$$

Where, $Q_H$ was the charges due to hydrogen desorption, and [Pt] represented Pt loading on anode.

Another CV scan was conducted in a standard three-electrode cell. The CV scan was measured to compare the activity of the two homemade catalysts [18]. The glassy carbon disk (3 mm diam, CH Instrument, Inc) covered with catalyst was used as working electrode. 5μL of ultrasonically re-dispersed catalyst suspension (2 mg mL$^{-1}$) was spread on the glassy carbon disk. After drying in vacuum, the obtained electrode was coated with 5μL of 5 wt % Nafion solution to form a Nafion film. The counter electrode was platinum foil (1 cm$^2$). The reference electrode was a reversible hydrogen electrode (RHE). The CV scans were performed in the electrolyte of 0.5 mol L$^{-1}$ $H_2SO_4$ containing 1.5 mol L$^{-1}$ DME between 0.05 and 1.2 V (versus the RHE) at 25 $^o$C. The scan rate was 0.05 V s$^{-1}$.

### 2.4.2. Fuel cell tests.

The performances of MEAs fabricated with different anodic catalyst were tested by Arbin Fuel Cell Testing System at 70 $^o$C. The 1.5mol L$^{-1}$ DME solution was the anodic fuel. The flow rate of DME solution was 3 mL min$^{-1}$. The humidified oxygen (200 mL min$^{-1}$) was fed to the cathode side under ambient pressure

## 3. RESULTS AND DISCUSSION

TEM images and the corresponding histograms of $Pt/SnO_2/C$ and Pt/C are presented in Fig. 1 and Fig. 2. The corresponding histograms are obtained by random measurements of 200 Pt nanoparticles. The Pt particles are uniformly dispersed on $SnO_2/C$ and carbon black supports. The average sizes of Pt

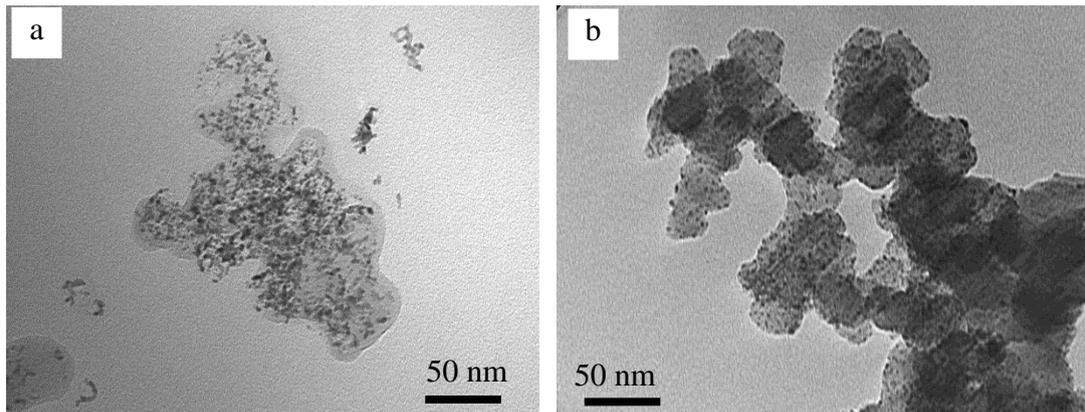particles are nearly the same (3.2 nm) for the two catalysts.



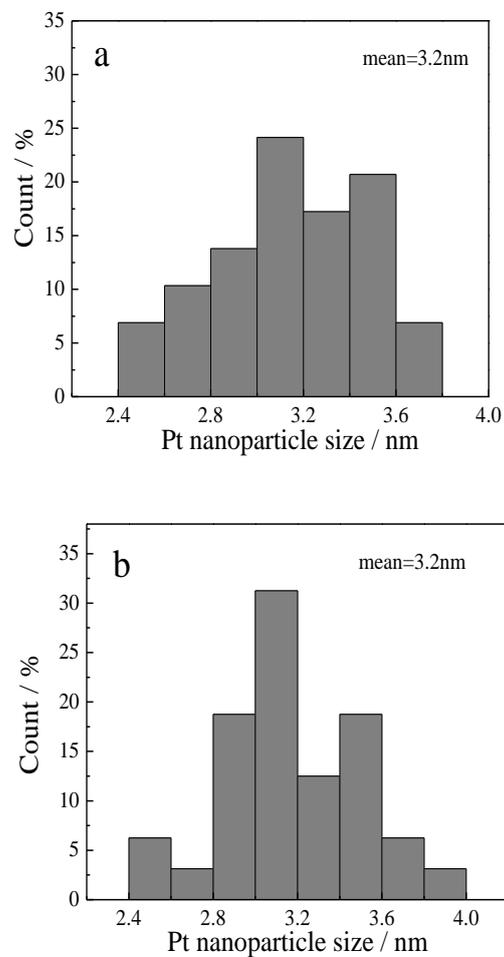**Figure 1.** TEM images of Pt/SnO$_2$/C and Pt/C catalysts: (a) Pt/SnO$_2$/C; (b) Pt/C.



**Figure 2.** Size distribution of Pt/SnO$_2$/C and Pt/C catalysts: (a) Pt/SnO$_2$/C; (b) Pt/C.

The compositions of the Pt/SnO$_2$/C and Pt/C are analyzed by EDAX. The Pt content of Pt/SnO$_2$/C and Pt/C catalyst is 17.88 *wt*% and 18.42 *wt*%, respectively, which are approximately equal to the

theoretical Pt content in catalyst (20 *wt*%). The content of $SnO_2$ in prepared $SnO_2$/C composite is 18.60 *wt* %, which is almost equal to the theoretical value (20 *wt*%).
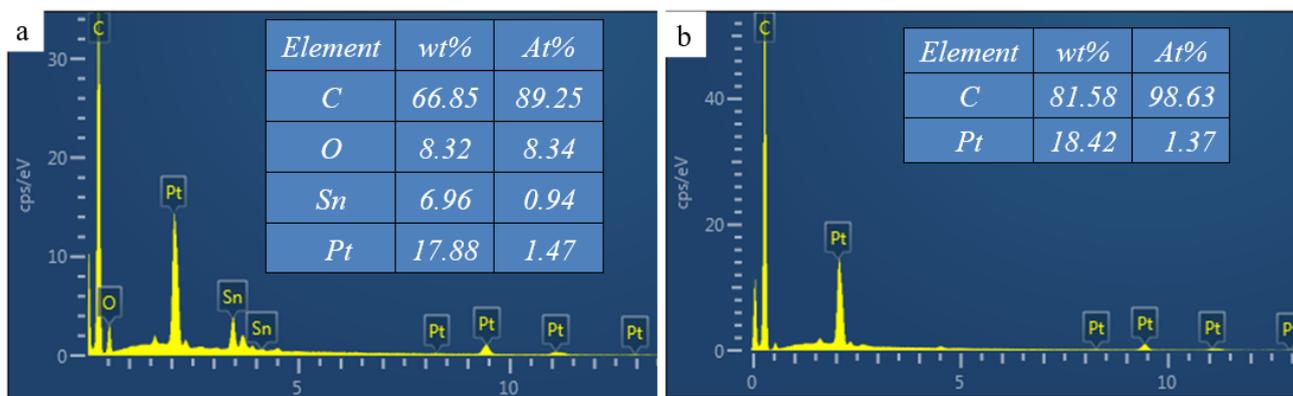


**Figure 3** EDAX patterns of Pt/SnO$_2$/C and Pt/C catalysts and their quantitative analysis: (a) Pt/SnO$_2$/C; (b) Pt/C.

To compare the activity of Pt/SnO$_2$/C and Pt/C for DME oxidation, the cyclic voltammograms are recorded in 0.5 mol L$^{-1}$ H$_2$SO$_4$ + 1.5 mol L$^{-1}$ DME solution. The onset potential of DME oxidation on Pt/SnO$_2$/C is about 0.55 V.
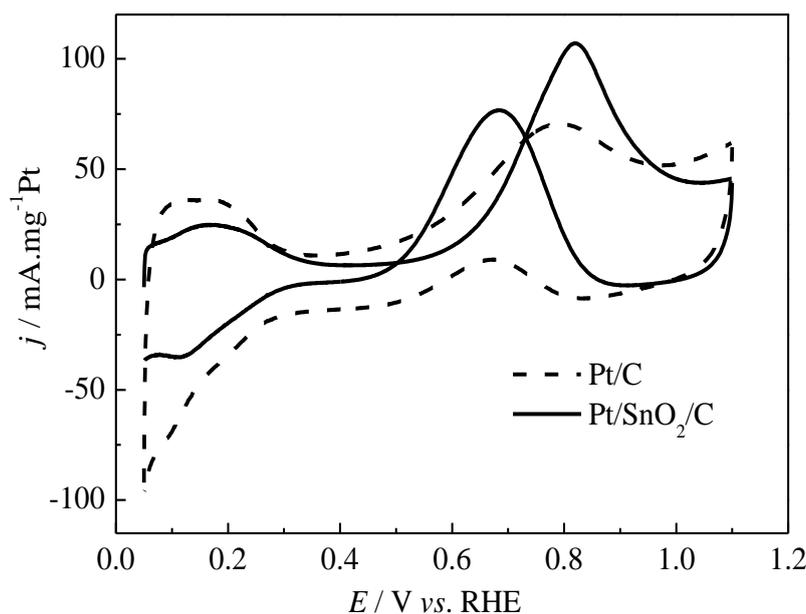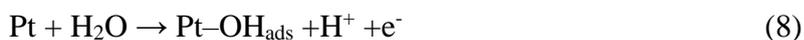


**Figure 4.** Cyclic voltammograms of DME electrooxidation in 0.5 mol L$^{-1}$ H$_2$SO$_4$ + 1.5 mol L$^{-1}$ DME aqueous solution on Pt/SnO$_2$/C and Pt/C catalysts. Scan rate: 0.05 V s$^{-1}$.

The peak current of DME oxidation on Pt/SnO$_2$/C is about 107 mA mg$^{-1}$ Pt, which is much higher than that of Pt/C (70 mA mg$^{-1}$ Pt). Thus, the Pt/SnO$_2$/C catalyst shows more excellent catalytic activity. G. Kerangueven [19] reports the CV curves of Pt-based catalysts in H$_2$SO$_4$ solutions with or without

DME. The peaks of CV curves with DME are suppressed during the $H_2$ adsorption and desorption potential range. The dissociative adsorption of DME suppresses $H_2$ adsorption and desorption in low potential range. Y. Liu [20] investigates the dissociative adsorption of DME and methanol in hydrogen range. The results show that both DME and methanol can absorb on catalyst and suppress the hydrogen adsorption and desorption reaction in low potential range. But the adsorption of DME is weaker than methanol. A fewer amount of DME molecules can be adsorbed and then dehydrogenated on catalyst compared with that of methanol. The activity of DME oxidation reaction is lower than methanol. The similar results have been reported by M. H. Shao [21], which use $HClO_4$ as the electrolyte. The improvement of the adsorption of DME on catalyst is very important for DDFC. As shown in Fig.4, the CV curve of $Pt/SnO_2/C$ has been suppressed during the $H_2$ adsorption and desorption potential range (from 0.03V to 0.28V). That is, the adsorption of DME on $Pt/SnO_2/C$ is easier than Pt/C in low potential range. The mechanism of DME electro-oxidation reported by Q. Zhang is as follows [22]:

$$CH_3-O-CH_3 + Pt \rightarrow Pt-C-O-CH_3 + H^+ + 2e^- \qquad (2)$$
$$CH_3-O-CH_3 + Pt \rightarrow Pt-(CHOCH)-Pt + 4H^+ + 4e^- \qquad (3)$$
$$Pt-C-O-CH_3 + H_2O \rightarrow Pt-COH + CH_3OH \qquad (4)$$
$$Pt-(CHOCH)-Pt + H_2O \rightarrow 2Pt-CO + 4H^+ + 4e^- \qquad (5)$$
$$Pt-COH \rightarrow Pt-CO + H^+ + e^- \qquad (6)$$
$$CH_3OH + Pt \rightarrow Pt-CO + 4H^+ + 4e^- \qquad (7)$$
$$Pt + H_2O \rightarrow Pt-OH_{ads} + H^+ + e^- \qquad (8)$$
$$Pt-CO + Pt-OH_{ads} \rightarrow CO_2 + H^+ + e^- \qquad (9)$$
$$Pt-COH + Pt-OH_{ads} \rightarrow CO_2 + H^+ + 2e^- \qquad (10)$$
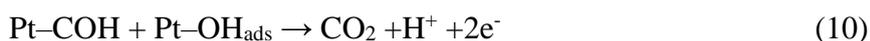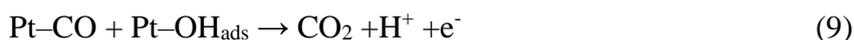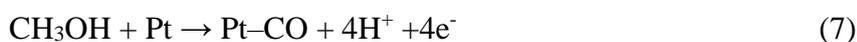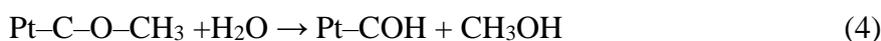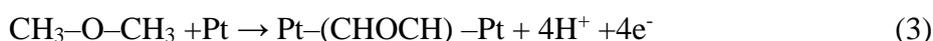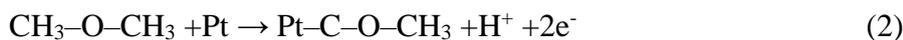
According to the above mechanism, the adsorption of DME on Pt is the first step of DME oxidation, which can significantly affect the reaction speed. $Pt/SnO_2/C$ is benefit to DME adsorption, which is a main cause for the increase in anodic catalyst activity. The IR spectra in Fig. 5 show the characteristic peak of $SnO_2$. The band in the range of 500-750 $cm^{-1}$ is due to the Sn-O vibration. The band at about 1600 $cm^{-1}$ is assigned to the bending vibration of O-H. The broad band at about 3430 $cm^{-1}$ is stretching vibration of O-H. As shown in Fig. 5, there are sufficient $OH_{ads}$ species existed on the surface of $SnO_2$. Many researchers have reported the intermediates generated during DME oxidation reaction. As shown in the Eq. (9) and (10), –CO and –COH are the poisoning intermediates adsorbed on Pt. Besides, other researchers consider that $-CH_2OCH_3$, -COOH and formaldehyde are the possible intermediates of DME oxidation reaction [21,23,24]. The $OH_{ads}$ species on the surface of $SnO_2$ promote the oxidation of intermediates species which benefits to reduce the Pt poisoning effect and release Pt active sites. The dehydrogenation of DME on Pt surface needs three adjacent Pt active sites. The elimination of adsorbed intermediates species can increase the amount of adjacent Pt active sites, which is another cause for the increase in anodic catalyst activity.
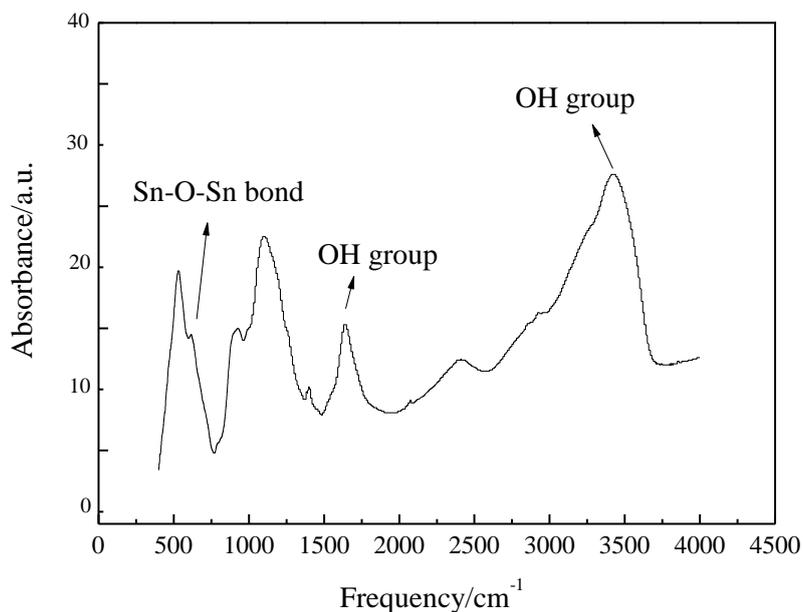
**Figure 5.** IR spectra of SnO₂ particles after dehydration treatment at 200 °C under vacuum condition.

Fig. 6 shows the polarization curves and the power density curves of MEAs with different anodic catalyst at 70 °C. The maximum power density of the MEAs with Pt/SnO₂/C and Pt/C anodic catalyst is 49.6 mW cm⁻² and 33.6 mW cm⁻², respectively. Obviously, DDFC with Pt/SnO₂/C anodic catalyst obtains higher output performance. Pt/SnO₂/C is a proper anodic catalyst for DME, which can enhance the output performance of DDFC. The performances of DDFCs with different anode catalysts have been reported in many published literatures. The comparison of these works is listed in table 1[18,25-27]. Comparing to these works in table 1, the performance of DDFC with Pt/SnO₂/C anode catalyst is obvious higher at relatively low temperature (70 °C) and under relatively low pressure (1 bar).
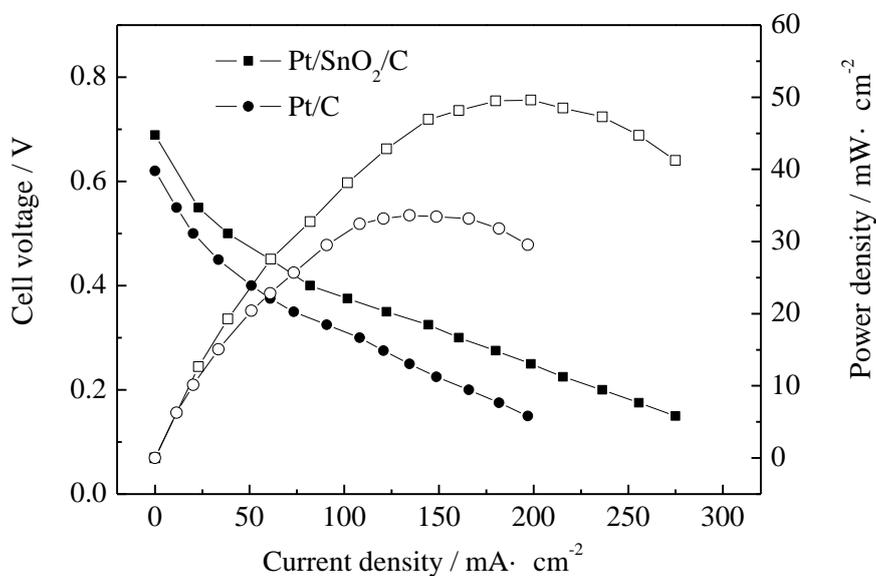


**Figure 6.** The polarization curves and the power density curves of the MEAs with various anode catalysts at 70 °C.

**Table 1.** The performances of DDFCs with different anode catalysts reported in literatures and this work

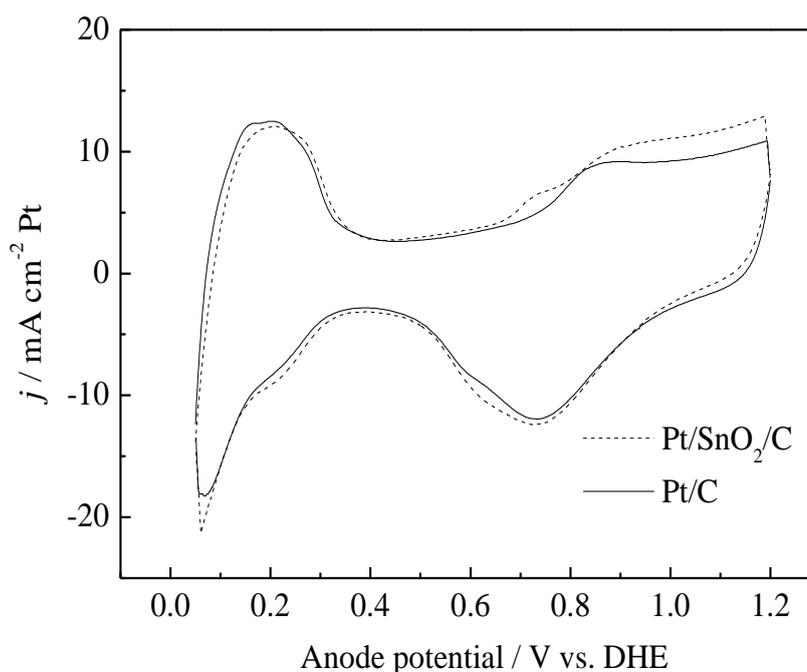|   | Catalyst | The maximum power density/ mW cm$^{-2}$ | Temperature/ °C | Pressure/bar | Reference |
|---|----------|------------------------------------------|------------------|--------------|-----------|
| 1 | PtCu | 13.5 | 80 | 1 | 7 |
| 2 | Pt/C | 60 | 80 | 3 | 8 |
| 3 | Pt/MWNT | 38.4 | 80 | 1 | 9 |
| 4 | PtRu | 38 | 80 | 1 | 10 |
| 5 | Pt/SnO$_2$/C | 49.6 | 70 | 1 | Present work |



**Figure 7.** Cyclic voltammograms of anodes with various catalysts at a scan rate of 0.01V s$^{-1}$, in a potential range between 0.05 and 1.2V vs. DHE.

Fig.7 presents the anodic *EAS* of MEAs with different catalyst. The anodic *EAS* of MEA with Pt/SnO$_2$/C catalyst is 81 m$^2$ g$^{-1}$Pt. The anodic *EAS* of the other MEA is 87 m$^2$ g$^{-1}$Pt. The *EAS* of different MEAs are nearly the same. The value of *EAS* represents the amount of Pt active sites in anode. That is, the MEAs with different catalyst have nearly the same amount of anodic Pt active sites. The enhancement of DDFC performance can be ascribed to the higher activity of anode catalyst.

# 4. CONCLUSIONS

Pt/SnO$_2$/C catalyst with SnO$_2$/C as its supports has been prepared for DME electrooxidation in an acidic medium. TEM tests show that the average sizes of Pt particles are nearly the same (3.2 nm) for Pt/SnO$_2$/C and Pt/C. The Pt/SnO$_2$/C catalyst shows higher activity than Pt/C towards DME oxidation.

The adsorption of DME on Pt/SnO$_2$/C is easier than Pt/C, which promotes the oxidation of DME. IR spectra results show that there are sufficient OH$_{ads}$ species existed on the surface of SnO$_2$. These OH$_{ads}$ species benefit to reduce the Pt poisoning effect and release Pt active sites. The maximum power density of DDFC with Pt/SnO$_2$/C anodic catalyst is higher than DDFC with Pt/C anodic catalyst. DDFCs with different anodic catalyst have nearly the same anodic *EAS*. Therefore, the enhanced performance is attributed to the higher activity of Pt/SnO$_2$/C for DME oxidation.

**References**

1. L.Z. Yin, Q. Li, W.R. Chen, T.H. Wang, and H. Liu, *Int. J. Hydrogen Energy*, 11 (2019) 5499.
2. K.J. Reddy, and N. Sudhakar, *Int. J. Hydrogen Energy*, 44 (2019) 15355.
3. G.H. Gwak, D.H. Kim, S. Lee, and H. Ju, *Int. J. Hydrogen Energy*, 43 (2018) 13999.
4. C. Ouyang, X.L. Zhang, M.F. Wu, D.M. Xun, and P.P. Gao, *Int. J. Electrochem. Sci.*, 15 (2020) 80.
5. Y. Zhao, L.W. Chen, and Y.D. Meng, *Int. J. Electrochem. Sci.*, 14 (2019) 6826.
6. L.H. Xing, G.P. Yin, Z.B. Wang, S. Zhang, Y.Z. Gao, and C.Y. Du, *J. Power Sources*, 198 (2012) 170.
7. J.H. Yu, H.G. Choi, and S.M. Cho, *Electrochem. Commun.*, 7 (2005) 1385.
8. L. H. Xing, Y.Z. Gao, Z.B. Wang, C.Y. Du, and G.P. Yin, *Int. J. Hydrogen Energy*, 36 (2011) 11102.
9. U. Mondal, and G.D. Yadav, *J. CO$_2$ Util.*, 42 (2019) 16695.
10. W.J. Yuan, Y.F. Zhang, N.Y. Zhang, C.W. Yin, X.L. Zhang, and X.W. Liu, *Catal. Commun.*, 100 (2017) 66.
11. H. Zhang, C. Hu, X. He, L. Hong, G. Du, and Y. Zhang, *J. Power Sources*, 196 (2011) 4499.
12. W.Z. Hung, W.H. Chung, D.S. Tsai, D.P. Wilkinson, and Y.S. Huang, *Electrochim. Acta*, 55 (2010) 2116.
13. M.L. Dou, M. Hou, D. Liang, W.T. Lu, Z.G. Shao, and B.L. Yi, *Electrochim. Acta*, 92 (2013) 468.
14. Y. Fan, J.H. Liu, H.T. Lu, P. Huang, and D.L. Xiu, *Electrochim. Acta*, 76 (2012) 475.
15. N. Zhang, S. Zhang, C.Y. Du, Z.B. Wang, Y.Y. Shao, and K.F. Dong, *Electrochim. Acta*, 117 (2014) 413.
16. L.H. Xing, Z.B. Wang, C.Y. Du, and G.P. Yin, *Int. J. Energy Res.*, 36 (2012) 886.
17. L.H. Xing, G.P. Yin, C.Y. Du, S.X. Cui, M.H Zuo, and H.P. Wang, *Int. J. Hydrogen Energy*, 42 (2017) 16695.
18. K.D. Cai, G.P. Yin, J.J. Wang, and L.L. Lu, *Energy Fuels*, 23(2009) 903.
19. G. Kerangueven, C. Coutanceau , E. Sibert, J.M. Leger, and C. Lamy, *J. Power Sources,* 157 (2006) 318.
20. Y. Liu, M. Muraoka, S. Mitsushima, K.I. Ota, and N. Kamiya, *Electrochim. Acta,* 52 (2007) 5781.
21. M.H. Shao, J. Warren, N.S. Marinkovic, P.W. Faguy, and R.R. Adzic, *Electrochem. Commun.,* 7 (2005) 459.
22. Q. Zhang, Z.F. Li, S.W. Wang, W. Xing, R.J. Yu, and X.J Yu, *Electrochim. Acta,* 53 (2008) 8298.
23. G. Kerangueven, C. Coutanceau, E. Sibert, F. Hahn, J.M. Leger, and C. Lamy, *J. Appl.*

*Electrochem.*, 36 (2006) 441.
24. I. Mizutani, Y. Liu, S. Mitsushima, K.I. Ota, and N. Kamiya, *J. Power Sources*, 156 (2006) 183.
25. B. Gavriel, R. Sharabi, and L. Elbaz, *ChemSusChem*, 10 (2017) 3069.
26. L. Du, S.F Lou, G.Y Chen, G.X. Zhang, F.P Kong, Z.Y. Qian, C.Y. Du, Y.Z Gao, S.H. Sun, and G.P. Yin, *J. Power Sources,* 433 (2019) 126690.
27. J.Y. Im, B.S. Kim, H.G. Choi, and S.M. Cho, *J. Power Sources,* 179 (2009) 301.